Multi-Carrier Compressed Sensing Multi-User Detection System: A Practical Verification

Matthias Woltering, Fabian Monsees, Carsten Bockelmann and Armin Dekorsy
University of Bremen, Bremen, Germany
Email: {woltering, monsees, bockelmann, dekorsy}@ant.uni-bremen.de

***Abstract*—MCSM is a recently proposed novel system concept to solve the massive access problem envisioned in future communication systems like 5G and industry 4.0 systems. This work focuses on the practical verification of the theoretical gains that MCSM provides using a Hardware-In-the-Loop (HIL) measurement setup. We present results in two different scenarios: (i) a LoS lab setup and (ii) a non-LoS machine hall. In both scenarios MCSM shows promising performance in terms of the number of supported users and the achieved reliability.**

***Index Terms*—Massive Access, Compressive Sensing, Multi-carrier scheme, Activity Detection**

I. Introduction

Massive Machine-to-Machine (M2M) communication is expected to be one of the major drivers for new radio access technologies in the development of the 5th generation mobile networks (5G) as well as industrial radio systems for industry 4.0 (I4.0). For cellular networks forecasts indicate that in 2020 a factor 10 to 100 more machine type devices (MTD) than personal mobile phones will be served by a single base station with the number of MTDs connected in the range from 10.000 to 100.000 [1]–[3]. Similarly, the number of devices in industrial contexts will also grow tremendously given the needs of future I4.0 factories. While most current standards like UMTS/LTE or WLAN were conceived for relatively few devices with high data rates, a single MTD often only generates small amounts of user data, shows very diverse channel access or traffic patterns (triggered, periodically, sporadic or random), and for some applications also needs to be low-cost and very energy efficient to operate for long-lifetimes. As a consequence, new radio access technologies are required that are capable of supporting a variety of requirements. On the one hand massive access requires lean signaling and access structures; on the other hand, strict latency or reliability requirements need to be considered. Thus, PHY and MAC technologies with low signaling overhead and adaptable reliability, e.g., in terms of error protection, need to be designed for handling low data rate sporadic machine type communication (MTC) balancing the payload to overhead ratio as well as the reliability. To this end, we recently proposed the so-called multi-carrier compressed sensing multi-user detection (MCSM) system [4] which specifically addresses massive access, bandwidth efficiency and flexible bandwidth allocation out of the many challenges in MTC design. Theoretical work on MCSM has shown promising performance in terms of error rates and the number of connected devices, but practical verification in different scenarios was still missing. The focus of this work is a measurement campaign to show the performance of the proposed MCSM system by a Hardware-In-the-Loop (HIL) setup.

II. A Multi-Carrier System for Machine Type Communication

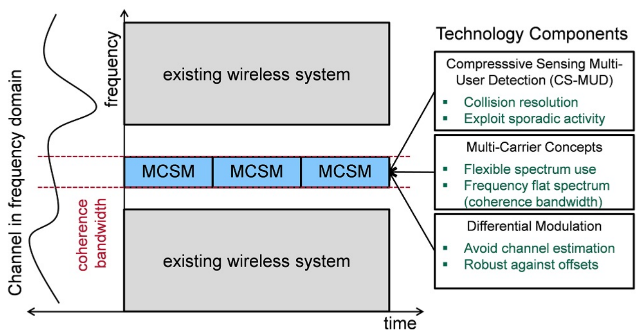

Fig. 1. Multi-Carrier Compressed Sensing Multi-User Detection (MCSM) concept and components.

Future solutions for either 5G MTC or I4.0 need to fulfill a number of basic requirements that strongly influence the design. First, coexistence has to be guaranteed. In a 5G context coexistence with other services like broadband access is crucial, whereas in I4.0 coexistence with other wireless systems in the same frequency band has to be ensured. Furthermore, we focus on the basic MTC requirements of low signalling overhead, high reliability and flexible resource use with a special attention on large number of served users. The recently proposed MCSM system [4], [5] tackles these MTC requirements by combining three different technology components as depicted in Figure 1: (i) multi-carrier concepts, (ii) compressive sensing multi-user detection (CS-MUD) and (iii) differential modulation. Each component will be discussed in more detail in the following section.

A. MCSM Components

1) Multi-Carrier Modulation: For flexible spectrum allocation multi-carrier systems with carefully designed waveforms have been identified as a potential solution [6]. On the one hand, coexistence management is enabled by good spectral containment; on the other hand, spectrally efficient multi-user approaches can be used for low-overhead direct random access communication. Thus, the first technology component of MCSM is a suitable multi-carrier concept to flexibly allocate spectrum for multiple

MCSM systems in one frequency band. In this paper we restrict to Orthogonal Frequency Division Multiplexing (OFDM) as a multi-carrier scheme, but general waveforms providing better spectral containment are equally applicable. Assume that the bandwidth shown in Figure 1 is divided into overall N_{IFFT} sub-carriers with a sub-carrier spacing Δf. Then a subset of N_{sc} sub-carriers is allocated to one particular MCSM system. MCSM systems are narrow-band systems serving up to K nodes per system and several systems can coexist within a certain bandwidth by simply allocating non-overlapping sub-carrier blocks. This also enables blanking of sub-bands used by other communication systems. We restrict the following descriptions to a single MCSM system to ease notation. The most important design criterion in choosing N_{sc} determines the bandwidth of the MCSM system: in order to enable non-coherent detection, i.e. the third MCSM component, the bandwidth $N_{\mathrm{sc}}\Delta f$ has to be smaller than or equal to the coherence bandwidth of the wireless channel $B_{\mathrm{c}} \approx 1/\tau_{\mathrm{c}}$, where τ_{c} denotes the delay spread of the channel.

2) Compressive Sensing Multi-User Detection (CS-MUD): While multi-carrier modulation provides flexible spectrum allocation the physical channel access for each MCSM system has to be designed with very low signaling overhead. To this end, direct random access, i.e. the transmission of payload without a multi-transmission handshake to reserve resources beforehand, has been identified as a crucial component to enable massive access [4], [7]. The basis for MCSM is CS-MUD, which has been proposed in literature to achieve direct random access with good collision resolution [8]. CS-MUD is a multi-user detection scheme that exploits certain structures in the multi-user signal. In massive MTC it can be assumed that only a subset of all nodes is active at any time leading to so-called sporadic access of the nodes. This sporadic nature can be exploited at the receiver by modeling inactive nodes as transmitting zeros instead of modulation symbols, yielding an efficient joint detection of activity and user data [9]. The main advantage is a highly reduced signaling overhead compared to known techniques. In this context, sparse multi-user detection facilitating such a joint data detection and signal acquisition is a promising candidate for the application in 5G cellular networks [7], [8], [10].

3) Differential Modulation: In addition to CS-MUD a third component is required to lower the required signalling overhead even further. Many of todays communication systems employ coherent communication technologies to achieve high data rates at the cost of signalling, i.e. pilots are required for high quality channel estimation. However, differential modulation concepts like Differential M-Phase Shift Keying (D-MPSK) allow for a robust transmission without need for channel estimation as long as the channel can be assumed flat.

B. MCSM Node Processing and Detection Model

In the following receiver and transmitter side processing are shortly summarized. For a complete theoretical description please refer to [5].

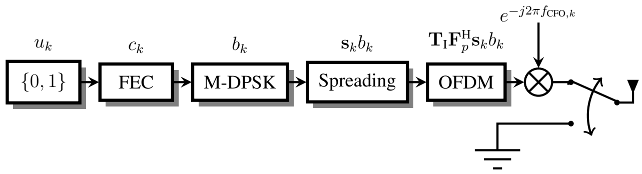

Fig. 2. Transmitter side processing at every MCSM node.

1) Transmitter (Node): Figure 2 shows the block diagram of a single node out of K nodes summarizing one MCSM system. Each node in an MCSM system can either be active or inactive. In the following, we describe the transmitter processing of an active node.

First, the N_{u} data bits $\mathbf{u} \in \{0,1\}^{N_{\mathrm{u}}}$ of a single node k are protected by a forward error correcting code and are modulated according to a D-MPSK modulation. In particular, the encoded information sequence $\mathbf{c} \in \{0,1\}^{N_{\mathrm{c}}}$ will be modulated to a M-Phase Shift Keying (M-PSK) alphabet resulting in symbols $\mathbf{a} \in \mathbb{C}^{N_{\mathrm{a}}}$, where N_{a} denotes the frame length. These symbols are differentially modulated to a so called D-MPSK signal through $b_k(i) = a_k(i)b_k(i-1)$, where i denotes the symbol clock and a known starting phase such as $b_k(0) = 1$ is assumed. In the following we restrict ourselves to the case that a MCSM node k spreads each differentially modulated symbol $b_k(i)$ to one OFDM symbol consisting of N_{sc} sub-carriers by using a unique node-specific spreading sequence $\mathbf{s}_k \in \mathbb{C}^{N_{\mathrm{s}}}$ that is known at the base station [11]. In this case we have $N_{\mathrm{s}} = N_{\mathrm{sc}}$ and the symbol clock i remains unchanged for the OFDM symbols. Note that other constellations are possible. The spread frequency domain symbol is then converted to a time domain symbol via a partial IDFT matrix $\mathbf{F}_p^{\mathrm{H}} \in \mathbb{C}^{N_{\mathrm{IFFT}} \times N_{\mathrm{sc}}}$ such that the node occupies only the N_{sc} out of N_{IFFT} sub-carriers allocated to that particular MCSM system. Subsequently, a cyclic prefix (CP) is added in time domain by multiplication with a matrix $\mathbf{T}_{\mathrm{I}}$ to counteract inter-symbol interference. Thus, the transmit signal vector $\mathbf{x}_k(i)$ of node k in time domain is formally

$$\mathbf{x}_k(i) = \mathbf{T}_{\mathrm{I}}\mathbf{F}_p^{\mathrm{H}}\mathbf{s}_k b_k(i) \tag{1}$$

2) Receiver Processing (Access Point): The MCSM detection model employed at the base station contains the symbols of all K nodes in the system that are potentially active and superimposed in time domain. Active as well as inactive users are included in the detection model due to the unknown user activity. Assuming a frequency flat fading channel over the allocated N_{sc} sub-carriers (coherence bandwidth) with the convolutional channel matrix $\mathbf{H}_k$ for user k, the received signal after removing the CP in time domain with $\mathbf{T}_{\mathrm{R}}$ and transforming into the frequency domain by $\mathbf{F}_p$ at the base station for the i-th symbol is

$$\mathbf{y}(i) = \sum_{k=1}^{K} \underbrace{\mathbf{F}_p \mathbf{T}_\mathrm{R} \mathbf{H}_k \mathbf{T}_\mathrm{I} \mathbf{F}_p^\mathrm{H}}_{h_k \mathbf{I}_p} \mathbf{s}_k b_k(i) \tag{2}$$

Here, $\mathbf{F}_p \mathbf{T}_\mathrm{R} \mathbf{H}_k \mathbf{T}_\mathrm{I} \mathbf{F}_p^\mathrm{H} = h_k \mathbf{I}_p \in \mathbb{C}^{N_\mathrm{sc} \times N_\mathrm{sc}}$ denotes a frequency flat fading channel with a single node specific channel tap h_k. Furthermore, the user symbols $b_k(i)$ can be either D-MPSK or zero modeling the inactivity, and $\tilde{b}_k(i) = b_k(i) h_k$ is the differentially modulated symbol weighted with the node specific channel coefficient. Hence, we can write the received signal in frequency domain in matrix form as

$$\mathbf{y}(i) = \mathbf{S}\tilde{\mathbf{b}}(i) \tag{3}$$

where $\tilde{\mathbf{b}}(i) \in \mathbb{C}^{K \times 1}$ contains the differentially modulated symbols from all K nodes weighted with the individual channel taps or zeros for inactive users. The matrix $\mathbf{S} \in \mathbb{C}^{N_\mathrm{sc} \times K}$ contains the spreading sequences $\mathbf{s}_k$ of all K nodes as column vectors. For a whole transmit frame, of N_a symbols, we can write

$$\mathbf{Y} = \mathbf{S}\tilde{\mathbf{B}} \tag{4}$$

where $\mathbf{Y} \in \mathbb{C}^{N_\mathrm{sc} \times N_\mathrm{a}}$ and $\tilde{\mathbf{B}} \in \mathbb{C}^{K \times N_\mathrm{a}}$ summarize the received and transmitted frame, respectively. The block

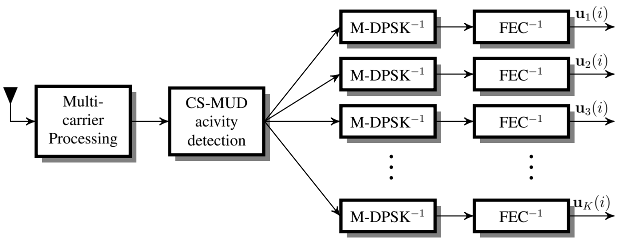

Fig. 3. Base Station processing.

diagram of the base-station processing is exemplary shown in Figure 3. After converting the time domain symbols to frequency domain leading to (4) Compressed Sensing algorithms are employed to solve the sparse and underdetermined set of equations. While other algorithms are possible, we apply a Group Orthogonal Matching Pursuit (GOMP) as Compressed Sensing algorithm to detect the activity of the nodes.

The GOMP performs two steps consecutively: first it estimates the activity of one node and, subsequently, estimates the data of that node. This procedure is repeated until a certain stopping criterion is met. For a more detailed description of the GOMP the reader is referred to [12]. At the output of the GOMP, we have estimates $\hat{b}_k(i)$ for the modulated symbols of the active nodes. The receiver recovers the modulation symbols by performing differential demodulation

$$\hat{a}_k(i) = \frac{\hat{b}_k(i)}{\hat{b}_k(i-1)} = \hat{b}_k(i)\hat{b}_k^*(i-1) \tag{5}$$

which are subsequently demapped to the code word estimate $\hat{\mathbf{c}}_k$. Finally, the estimated information bit sequence $\hat{\mathbf{u}}_k$ is obtained by decoding the code word. Please note that this is the simplest form of a D-MPSK demodulator and more advanced techniques exist but are out of the scope of this paper.

III. Measurement Setup

A practical measurement with a simplified transmission scenario is implemented to evaluate the proposed MCSM system. Two development hardware platforms serve as measurement environment. First, the platforms, the frame structure and the modeling of the massive access will be introduced. Then, we shortly describe the two different measurement scenarios: 1) A Line of Sight (LoS) setup within our laboratory and 2) a non-Line of Sight (non-LoS) setup in a machine hall, where different interference factors like metal switch cabinets, machines and material affect the transmission.

A. Hardware Platform and Setup

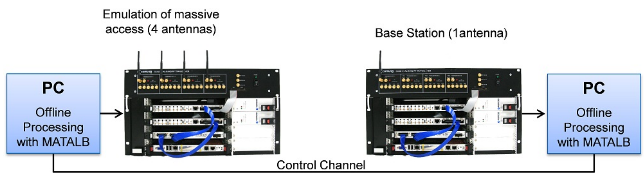

Fig. 4. Hardware-in-the-Loop (HIL) setup.

Both Nutaq hardware development platforms used in our measurement setup are equipped with an 8 channel 14 Bit AD converter with up to 125 Mega Samples per second (MSPS) as well as an 8 channel 14 Bit DA converter with up to 500 MSPS. The maximum sampling rate is 104 MHz, which is decreased to 26 MHz for this measurement due to memory bandwidth limitations. Hence, a sample timing of $T_\mathrm{s} = \frac{1}{26\mathrm{MHz}} = 38.462\mathrm{ns}$ results. Furthermore, both transceivers with four RF front-ends provide 26 dBm maximum transmission power for MIMO transmission within the 2.4 GHz and 5 GHz ISM Bands. The RF front-end is implemented as a non-DC-coupled high pass, where all frequencies larger 100 Hz up to a maximum bandwidth of 20 MHz pass the front-end. The typical CFO is specified as 100 ppm of the actual carrier frequency. Assuming an ISM Band with a carrier frequency $f_\mathrm{lo} = 2.4\mathrm{GHz}$ a CFO of approx. $f_{\mathrm{CFO},\iota} \approx \pm 2.4\mathrm{kHz}$ per transceiver is expected. During operation CFOs of up to $f_\mathrm{CFO} = |(f_\mathrm{lo,Tx} + f_\mathrm{CFO,Tx}) - (f_\mathrm{lo,Rx} + f_\mathrm{CFO,Rx})| \approx 5\mathrm{kHz}$ can be observed, which is well within specifications. Furthermore, both platforms contain a Windows PC that controls the hardware environment and facilitates the offline processing of the HIL setup using MATLAB. A direct Ethernet connection between both platforms simulates an ideal feedback control channel to enable automated measurements and error rate calculations.

B. Frame Structure and Emulation Massive Machine Access

The practical evaluation of massive access faces the challenge to realize a massive number of nodes that access a common base station. As illustrated in Figure 4 the two available transceivers are setup as HIL-devices: one serve as base station (RX), the other servers as a "user emulator" (TX). The base station processing is relatively straightforward along the lines described in section II-B with additional steps to ensure synchronization, CFO estimation and so on. The "user emulation", however, requires the generation of many virtual users and their mapping to the available hardware, i.e. primarily the four available antennas to emulate channel variations.

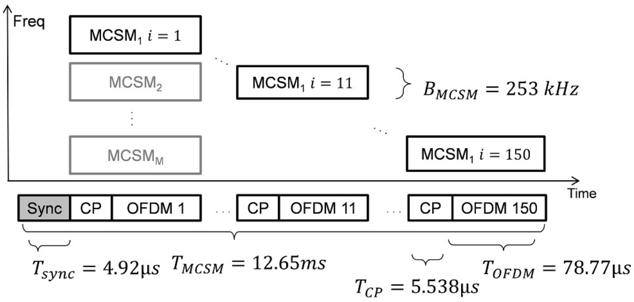

Fig. 5. Frame design and symbol timing.

1) Frame Structure and Node Parameters: The overall frame structure of our MCSM system is depicted in Figure 5. Multiple MCSM systems occupy the available 20MHz bandwidth at a carrier frequency of $f_{\text{lo}} = 2.484$ GHz. As a starting point to show the massive access capabilities of MCSM, we target an LTE like implementation. The upper part of Table I summarizes the resulting system parameters in comparison with LTE parameters. Additionally, Figure 5 shows the principle timing of one MCSM frame: the bandwidth is subdivided by an $N_{\text{IFFT}} = 2048$ point-IFFT leading to a core symbol timing $T_{\text{OFDM}} = N_{\text{IFFT}}/26\text{MHz} = 78.77\mu s$ with a sub-carrier spacing $\Delta f = \frac{1}{T_{\text{OFDM}}} = 12.695\text{kHz}$. Additionally, the CP of length 144 adds $T_{\text{CP}} = 5.538\mu s$ to the overall OFDM symbol.

TABLE I

SYSTEM PARAMETERS: OFDM COMPARED TO LTE

Parameter	Var	MCSM	LTE
Carrier frequency	f_{lo}	2.484 GHz	see 3GPP LTE
Sampling Time	T_s	38.462 ns	32.552 ns
IFFT length	N_{IFFT}	2048	2048
OFDM Symbol time	T_{OFDM}	$78.77\mu s$	$66.6666\mu s$
CP length	N_{CP}	144	144/160 or 512
CP Symbol time	T_{CP}	$5.538\mu s$	$4.6875\mu s$
Sub-carrier spacing	Δf	12.69 kHz	15 kHz

Each MCSM system and the emulated nodes are parametrized according to Table II. Each node transmits N_u information bits encoded by a half rate convolutional encoder with generators $[5_8; 7_8]$. Due to the spreading a single symbol is transmitted per OFDM symbol

TABLE II

SYSTEM PARAMETERS: NODE PARAMETERS.

Parameter	Var	MCSM
# of users	K	60
# info bits	N_u	150
Channel code		Conv $[5_8, 7_8]$
Code Rate		0.5
Modulation		D-4PSK
# spreading length	N_s	20
Occupied bandwidth	B_{MCSM}	253kHz
OFDM symbols	N_{OFDM}	150

such that one MCSM block occupies an overall bandwidth of $B_{\text{MCSM}} = N_{\text{sc}}\Delta f = 253\text{kHz}$ and consists of 150 OFDM symbols. This gives a total frame length of $N_{\text{MCSM}} = N_a\,(N_{\text{IFFT}} + N_{\text{CP}}) = 328800$ sample points and a total frame duration of $T_{\text{Frame,MCSM}} = N_{\text{MCSM}}T_s = 12.65\text{ms}$, which is slightly longer than the LTE frame of $T_{\text{Frame,LTE}} = 10\text{ms}$. Additionally, a regular frequency hopping of the MCSM systems is applied every 10 OFDM symbol to exploit frequency diversity if the channel is not frequency flat or changing over time. Note that more general frequency hopping strategies can also be applied. To evaluate the start of one frame an LTE related synchronization sequence of 128 samples or $T_{\text{sync}} = 4.92\mu s$ is added to the frame. The virtual massive access of all nodes is realized at the transmitter (TX) seen in Figure 6. Here, all signals of every active node (highlighted) are

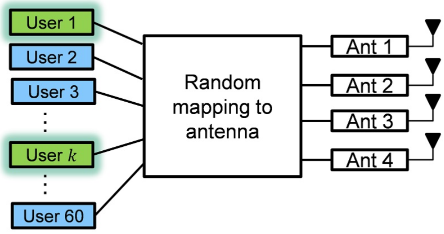

Fig. 6. Virtual massive access.

generated like described in (1). Each active node is randomly mapped to one antenna to emulate different user channels. The inactive nodes are modeled to be zero and therefore are not mapped to an antenna.

C. Measurement Environments

1) Setup 1: Line of Sight (LoS): Figure 7 shows the setup of the LoS scenario. The transmitter simulating the massive access (TX) is in the upper left, the receiver (RX) is located roughly 5 m away close to the door. The Line of Sight is unobstructed and mostly wooden furniture (some tables, cabinets, etc.) may act as scatters. Hence, the scenario is expected to show a mostly frequency-flat behavior which is reflected by the channel measurements depicted in Fig 8.

2) Setup 2: Non-Line of Sight (non-LoS): As a second setup we choose a more realistic industrial environment, i.e., a machine hall used for automation laboratories and

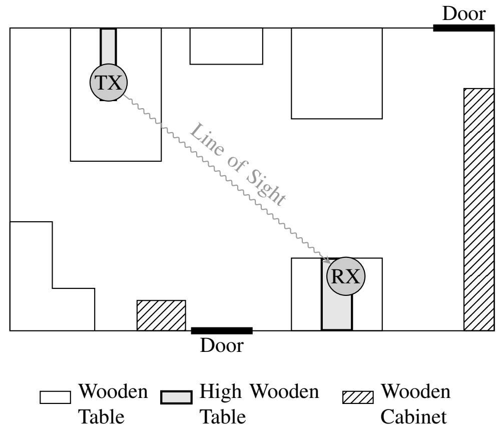

Fig. 7. LoS scenario: Schematic of the laboratory setup.

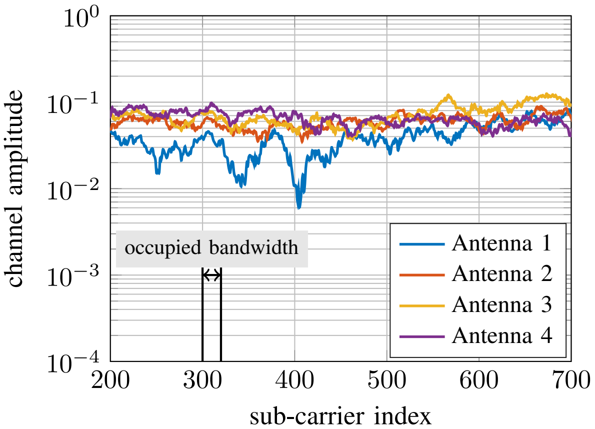

Fig. 8. LoS scenario: exemplary channel measurement with sub-carrier 200 up to 700 and the bandwidth of the MCSM system considered.

Fig. 9. Non-LoS scenario: Schematic of the machine hall setup

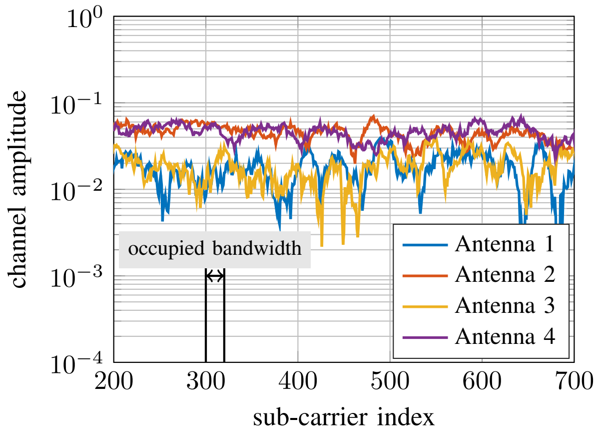

Fig. 10. Non-LoS scenario: exemplary channel measurement.

research. Figure 9 shows a picture of the scenario. The TX and the RX are located as far away as possible, which leads to a larger distance of roughly 14.5 m. Furthermore, the Line of Sight is now obstructed by metal switch cabinets, metal machines and other electrical components that are located within this hall. In addition to the setup 1 with only wooden cabinets and tables a high degree of reflections and stronger dampening of the signal is to be expected. Hence, the measured channel seen in Figure 10 is much more frequency selective.

IV. Measurement Results

Figure 11 shows the results of our measurements. The plot depicts the frame error percentage for different node activities at a fixed transmit power in the LoS case (setup 1). We see that MCSM performs highly reliable if up to 10 nodes are simultaneously active. Increasing the number of active nodes gracefully increases the likelihood for frame errors due to the higher system load. In setup 1 MCSM is mainly limited by the node activity due to the frequency flat channel and sufficiently high received power. To support higher number of active nodes, the MCSM parametrization can be adapted towards longer spreading codes and higher bandwidth allocation.

In contrast, Figure 12 shows the average frame error rate (FER) performance of MCSM in a non-LoS scenario (setup 2) with random node activity. The nodes are active with probability $p_a = 0.1$, which means we have $p_a K = 0.1 \cdot 60 = 6$ simultaneously active nodes on average using 253 kHz in a single MCSM system. In setup 2 the influence of different transmit powers can be observed due to the multi-path channel and the additional path loss compared to the LoS setup. For low transmit powers the FER is severely degraded but for high transmit powers a comparable performance to the LoS setup is achievable. For maximum transmit power of 26 dBm no errors could be observed during our measurement. Naturally, the coverage of any MCSM system given a minimum required reliability is strongly coupled with the propagation environment and allowed transmit powers.

V. Conclusion

In this work we have presented a practical evaluation of the MCSM system concept in a lab environment as well as a more realistic machine hall setup. Our measurements validate the theoretical findings of previous works with respect to the robustness and flexibility of the scheme. The presented results are only one exemplary MCSM parametrization which is specifically tuned to support a

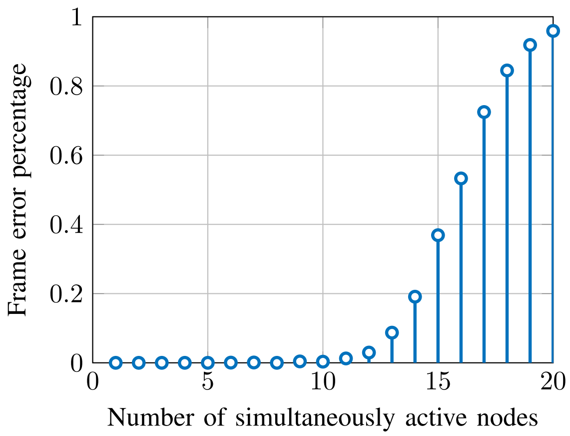

Fig. 11. Measured frame error percentage vs. the number of active users in LoS setup.

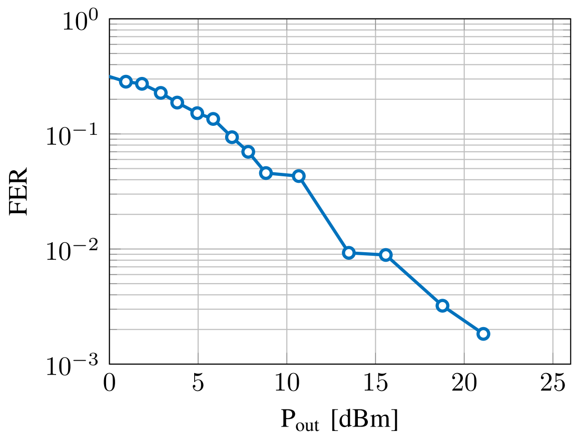

Fig. 12. Frame Error Rate vs. transmit power in non-LoS setup with random node activity.

high number of potential users in massive M2M situations. Furthermore, other parametrization can be tuned towards latency reduction (frame length) and higher reliability, e.g. by longer spreading sequences or by using stronger codes. In conclusion we have shown that the recently introduced MCSM system can be considered as a candidate technology for novel MTC applications in 5G and I4.0 applications.

References

[1] NGMN 5G Initiative, "5G White Paper," Feb. 2015.

[2] S. Y. Lien, K. C. Chen, and Y. Lin, "Toward ubiquitous massive accesses in 3gpp machine-to-machine communications," in *IEEE Communications Magazine*, Apr. 2011, pp. 66–74.

[3] M. Hasan, E. Hossain, and D. Niyato, "Random Access for Machine-to-Machine Communication in LTE-advanced Networks: Issues and Approaches," in *IEEE Communications Magazine*, June 2013, vol. 51.

[4] F. Monsees, M. Woltering, C. Bockelmann, and A. Dekorsy, "Compressive Sensing Multi-User Detection for Multi-Carrier Systems in Sporadic Machine Type Communication," in *IEEE 81th Vehicular Technology Conference (VTC2015-Spring)*, Glasgow, Great Britain, May 2015, vol. 81.

[5] F. Monsees, M. Woltering, C. Bockelmann, and A. Dekorsy, "A Potential Solution for MTC: Multi-Carrier Compressive Sensing Multi-User Detection," in *The Asilomar Conference on Signals, Systems, and Computers*, Asilomar Hotel and Conference Grounds, USA, Nov 2015.

[6] METIS project, "D6.6: Final Report on the METIS System Concept and Technology Roadmap," April 2015.

[7] H. Schepker, C. Bockelmann, and A. Dekorsy, "Exploiting Sparsity in Channel and Data Estimation for Sporadic Multi-User Communication," in *10th International Symposium on Wireless Communication Systems (ISWCS 13)*, Ilmenau, Germany, Aug 2013.

[8] C. Bockelmann, H. Schepker, and A. Dekorsy, "Compressive Sensing based Multi-User Detection for Machine-to-Machine Communication," *Transactions on Emerging Telecommunications Technologies: Special Issue on Machine-to-Machine: An emerging communication paradigm*, vol. 24, no. 4, pp. 389–400, June 2013.

[9] H. Zhu and G. B. Giannakis, "Exploiting Sparse User Activity in Multiuser Detection," *IEEE Transactions on Communications*, vol. 59, no. 2, pp. 454–465, 2011.

[10] Y. Ji, Č. Stefanović, C. Bockelmann, and P. Popovski A. Dekorsy, "Characterization of Coded Random Access with Compressive Sensing based Multi-User Detection," in *IEEE Globecom 2014*, Austin, TX, USA, Dec 2014.

[11] S. Verdu, *Multiuser Detection*, Cambridge University Press, 1998.

[12] H. Schepker, C. Bockelmann, and A. Dekorsy, "Improving Greedy Compressive Sensing Based Multi-User Detection with Iterative Feedback," in *2013 IEEE 78th Vehicular Technology Conference (VTC2013-Fall)*, Las Vegas, USA, Sep 2013.